RSC Advances

ROYAL SOCIETY OF CHEMISTRY

www.rsc.org/advances

Graphical abstract

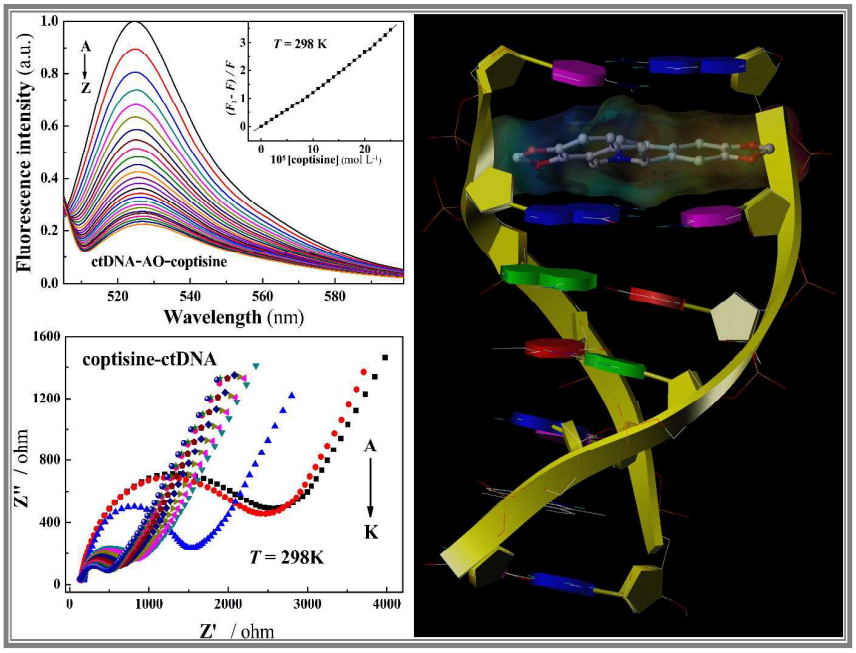

This study provides evidences of coptisine-DNA intercalation, which may help to develop new efficient, safe probes for the fluorometric detection of DNA instead of traditional toxic and carcinogenic probes.

Unraveling the Coptisine-ctDNA Binding Mechanism by Multispectroscopic, Electrochemical and Molecular Docking Methods

Ran Mi, Xiao-Ting Bai, Bao Tu, Yan-Jun Hu*

Hubei Collaborative Innovation Center for Rare Metal Chemistry, Hubei Key Laboratory of Pollutant Analysis & Reuse Technology, Department of Chemistry, Hubei Normal University, Huangshi 435002, PR China

Corresponding Author:

*Phone: +86–714–6515602. Fax: +86–714–6573832.

E–mail: yjhu@263.net (Y.J. Hu).

Abstract

Coptisine, an isoquinoline alkaloid, is an important medicinal herbal extract with diverse pharmacological and biological activities. Based on these considerations, an explorative study of the interaction of coptisine with calf thymus DNA (ctDNA) was conducted using multispectroscopic, electrochemical and molecular modeling techniques under simulative physiological conditions. Absorption spectra and iodide quenching experiments indicated that intercalation was the main DNA binding mode for coptisine. Fluorescence studies revealed that this interaction process is predominantly a dynamic process. This was further confirmed in a difference absorption spectrum and in electrochemical studies. The apparent activation energy, $E_{a,}$ remained largely constant at different temperatures. DNA chemical denaturation was used to further investigate the interaction and provided further support for the intercalation. Furthermore, the CD spectroscopy confirmed that coptisine not only interacted with the ctDNA, but it also perturbed ctDNA structure. In addition to experimental approaches, molecular modeling was used as a tool to verify and expand the experimental outcomes.

Keywords: Coptisine; ctDNA; Intercalation; Electrochemical methods; Molecular modeling

1. Introduction

Alkaloids are not only one of the most intensively studied classes of natural products, their wide spectrum of pharmacological activities also makes them indispensable drug ingredients in both traditional and modern medicine.[1–3] Coptisine (molecular structure: Figure 1), an isoquinoline alkaloid originally isolated from *Coptidisrhizoma*, *Chelidoniummajus* and *Corydalis uanhusuo,* is an important traditional medicinal herb and hasdemonstrates awide ranges of biological and pharmacological activities, including antimicrobial, antibacterial, anticancer, antidiarrhoeal, antioxidative and antidiabetic effects.[4–6] It also known to selectively inhibits proliferation of rat primary vascular smooth muscle cells.[7] As aqueous solutions of coptisine exhibit native fluorescence, it is also used as a fluorescent probe in biochemical research.[8–10]

Deoxyribonucleic acid (DNA) is an important genetic substance in organism. As a genetic instructor, DNA is involved in gene transcription, mutagenesis, gene expression, *etc*. and thus can be portrayed as one of the nature's most elementary conduits for the development and functioning of living organisms.[11] The action mechanisms of drugs are correlated with a drug binding process, which commonly involves the interaction of small drug molecules with large biomolecules, such as DNA, RNA or protein.[12] Recognition and characterization of the interaction mechanism between drugs and DNA is particularly valuable as they give effective information for designing new and more efficient therapeutic agents for the control of gene expression, along with providing an understanding of the reaction mechanism in question.[13–15] Consequently, binding studies of drugs with DNA are useful for understanding the reaction mechanism as well as for providing guidance for the application and design of new drugs. Usually, drugs bind to DNA under the following three dominant modes of interactions, (i) a small molecule ligand forms π–π stacking interactions between adjacent base pairs of DNA

(intercalative binding); (ii) the molecule binds the major or minor grooves involving van der Waals interactions (groove binding); and (iii) coulombic interactions occur between the negatively charged phosphate groups of DNA and cationic portion of the molecule (electrostatic binding).[15] Among these three types of binding, intercalative binding is the most effective for drugs targeting DNA.[16] However, it has been found that the factors that are responsible for intercalative binding are each of the three binding modes is quite complex. Hence, exploring the reaction modes and kinetic mechanisms between the different categories of molecules and DNA is very significant. In recent years, despite some researchers discussing the pharmacological activities of coptisine [4–6] and also developing various techniques to obtain biological interaction property,[17] the binding mechanism of coptisine-DNA has not been fully investigated at the molecular level.

In the present research, various instrumental techniques that have been used to study DNA-coptisine interactions, including UV-Visible absorbance, fluorescence spectroscopy, circular dichroism, electrochemical method and molecular docking. This combinatorial approach helps us to obtain a broader and more integrated range of information on the interaction between DNA and coptisine. Information regarding the binding mechanism, binding parameters, binding force and conformation are reported here. Our study provides evidences of coptisine-DNA intercalation, this finding may help to develop new efficient, safe probes for the fluorometric detection of DNA instead of traditional toxic and carcinogenic probes. Furthermore, the study of fluorescent moleculars is a very important research target for understanding biological events associated with interbiomolecular interactions.

2. Experimental

2.1 Materials

Calf thymus DNA (ctDNA) and tris (hydroxymethyl) aminomethane (Tris) were purchased from Sigma–Aldrich (St. Louis, MO); coptisine was obtained from Shanghai Jin Sui biological technology Co., Ltd (Shanghai, China); the sodium salt of ctDNA was used without further purification, since the purity was sufficiently high as determined from optical measurements; Tris buffer had a purity of no less than 99.5%, and all other reagents were of analytical purity. The ctDNA solution was dissolved in buffer solution, prior to storage at 4 ^{o}C for more than 12 h with gentle shaking to obtain homogeneity. The purity of ctDNA was verified by monitoring the ratio of absorbance at 260/280 nm (A260/A280), which was in the range 1.8–1.9.The concentration of ctDNA was determined by using an extinction coefficient of 6600 $mol^{-1}\cdot cm^{-1}$at 260 nm and expressed in terms of base molarity.[13] Ultrapure water was used throughout.

2.2 Apparatus

All fluorescence spectra were recorded on a Perkin-Elmer LS-55 luminescence spectrometer (PerkinElmer, Waltham, MA, USA) equipped with 1.0 cm quartz cells and a low temperature thermostatic bath (DFY–5/20, Shanghai Wei Kai Instrument Co. Ltd, China). The UV–vis absorption spectra were recorded at room temperature on a UV–9000S spectrophotometer (Metash, China) equipped with 1.0 cm quartz cells. Appropriate blanks corresponding to the buffer were subtracted to correct the fluorescence background. Circular dichroism (CD) spectra were measured with a Jasco J–810spectropolarimeter (Jasco, Tokyo, Japan) under constant nitrogen flush equipped with 1.0 cm quartz cells. The electrochemical experiments were performed on a CHI-660E electrochemical workstation (Chenhua Instruments Inc., Shanghai, China)

with a conventional three-electrode electrochemical testing system.

2.3 Measurements of spectrum

The UV–vis absorption spectra of ctDNA, coptisine alone, as well as the coptisine–ctDNA system, were measured from 200 nm to 600 nm. The solutions of the blank buffer and sample were placed in the reference and sample cuvettes respectively. The fluorescence spectra were performed at room temperature and at different temperatures (292, 298, 304, and 310 K). The slit widths for excitation and emission were set to 15.0 and 4.0 nm respectively. Titrations were performed manually by using trace syringes. For CD experiments, the concentration of ctDNA was kept at 1.0×10^{-4} mol·L^{-1}, while the concentration of coptisine was varied from 0 to 10.0×10^{-7} mol·L^{-1}, at increments of 2.0×10^{-7} mol·L^{-1}. The CD spectra were obtained employing a scanning speed of 100 nm/min from 220 to 320 nm in Tris–HCl (pH 7.2) at room temperature under constant nitrogen flush. Each spectrum was corrected with Tris–HCl buffer solution.

2.4 Electrochemical experiments

2.4.1 Preparation of electrode

The working electrode was a bare gold electrode (2 mm diameter), whereas the Ag / AgCl (3 mol·L^{-1} KCl) electrode served as the reference electrode and a platinum wire was used as the counter electrode. The bare gold electrode was polished to a mirror-like surface with 0.05 μm alumina slurry on micro–cloth pads, and was sonicated in acetone and ultrapure water for about 10 min respectively. Then it was dipped in 8 mL ctDNA solution (7.5×10^{-5} mol·L^{-1}) for several hours. After 24 h, the electrode was washed by ultrapure water several times and dried in nitrogen airflow and was then ready for use.

2.4.2 Cyclic voltammetry and electrochemical impedance spectroscopy

A conventional three electrode system was used, and all the measurements were carried out at room temperature. The electrolyte contains 5×10^{-3} mol·L^{-1} $K_3Fe(CN)_6$ / $K_4Fe(CN)_6$ (1:1) and 0.10 mol·L^{-1} KCl. 5 mL electrolyte was added into the electrochemical cell. The electrodes were immersed for measuring cyclic voltammetry curves over multiple scans until stabilized cyclic voltammograms were obtained. Following this, different concentrations of coptisine solution were added continuously to the system and stirred for 5 min, prior to resting for 3 min before testing. The cyclic voltammograms of the ctDNA modified gold electrode in the absence and the presence of drug were recorded at a scan rate of 0.1 V s^{-1}, the scan range was from –0.2 to 0.8 V. The electrochemical impedance spectra (EIS) were measured within the frequency range from 0.1 to 100 000 Hz and analyzed by Z–view software. The EISs of the bare ctDNA–modified Au electrode was measured multiple times to first obtain a baseline; then, different concentrations of coptisine solution were added continuously to the system to monitor the EIS. All measurements were repeated a minimum of three times to obtain meaningful results with different electrodes.

2.5 Molecular modeling

The 3D crystal structure of B–DNA used for docking was extracted from the RCSB Protein Data Bank (PDB), identifier 1Z3F. Molecular docking studies were conducted using the Surflex Dock program in the Sybyl–X 2.1.1 package.[18] Water was removed from the DNA PDB file. Polar hydrogen atoms and Gasteiger charges were added by AMBER7 FF99 method to prepare the DNA molecule for docking analysis. The protomol was generated in ligand mode with the Threshold was set at 0.50 and the Bloat was 0. The structure of coptisine was drawn in the Sybyl–X 2.1.1 package, polar H

added and being energy optimized with a tripos force field and charged optimized with Gasteiger–Huckel method. Ring flexibility was considered and other parameters during the docking program were determined through a number of attempts.

3. Results and discussion

3.1 Absorption spectra

UV–Vis absorption spectroscopy is perhaps the simplest and most commonly employed instrumental technique for studying both the stability of DNA and their interactions with small molecules. The study of drug–DNA interactions can be carried out by UV–Visible absorption spectroscopy through monitoring changes in the absorption properties of the drug or the DNA molecules.[19] In general, hyperchromism and hypochromism are regarded as spectral features for DNA double–helix structural change when DNA interacts with other molecules. The coptisine absorption studies were performed using ctDNA with the addition of varying concentrations of coptisine (Figure 2). The spectrum for free ctDNA shows a characteristic DNA absorption peak at $\lambda \approx 260$ nm and the characteristic coptisine absorption peaks at $\lambda \approx 260$ nm, 355 nm and 455 nm. The absorption peaks at 260 nm, 355 nm and 455 nm increased after the addition of different concentrations of coptisine. The inset in Figure 2 shows that the absorption value of free ctDNA and free coptisine was a little greater than the absorption value of the ctDNA–coptisine complex. This indicates that a weak hypochromic effect existed between ctDNA and coptisine, which is representative of coptisine intercalating between DNA base pairs. Seeing as the intercalative mode involves a π–π stacking interaction between an aromatic chromophore and the base pair of DNA, and the intercalating surface is sandwiched tightly between the aromatic, heterocyclic base pairs, as well as stabilized electronically in the helix, the strength of

this electronic interaction is expected to decrease as the cube of the distance between the chromophore and the DNA bases decreases. Thus intercalative binding commonly results in hypochromism.[20] The intercalative binding mechanism of coptisine with DNA is further corroborated in the experiments outlined below.

3.2 Fluorescence spectroscopy characteristics

Fluorescence spectroscopy is a commonly used technique in the study of interactions between small ligands and DNA due to its high sensitivity, large linear concentration range and selectivity.[21] The fluorescence band of free coptisine (λ_{ex} = 365 nm) was obtained at 450 nm, and upon gradual binding with ctDNA, the fluorescence intensity of the band gradually increased (Figure 3). The plot (Figure 3, inset) shows that when the concentration of coptisine was higher than 9.0×10^{-6} mol·L^{-1} the fluorescence intensity was constant. The experiment results indicated that the fluorescence of the system increased after coptisine binding to ctDNA, confirming that coptisine did bind ctDNA.

Because of the intrinsic weak fluorescence emission of ctDNA, acridine orange (AO), a common fluorophore that bind to DNA, was used to mark the DNA molecules. The fluorescene of AO increases in the presence of ctDNA, due to its strong intercalation between the adjacent ctDNA base pairs.[22] Thus if the coptisine molecule intercalates into ctDNA, a decrease in the fluorescence intensity of AO–ctDNA is expected, because it will compete with AO in binding with ctDNA. The emission spectra of the ctDNA–AO system (Figure 4) clearly decreased in the presence of coptisine. This result further validated that the coptisine molecule itself intercalates with ctDNA.

3.3 Iodide quenching experiment

To elucidate the intercalative binding of coptisine to ctDNA, fluorescence quenching in the presence and absence of ctDNA was examined using potassium iodide (KI) as a

quencher. As DNA contains a negatively charged phosphate backbone, a highly negatively charged quencher is expected to be repelled by DNA. Therefore, an intercalative-bound small molecule is protected in the presence of anionic quenchers. In case of groove binding, fluorescence quenching with anionic quenchers will be enhanced appreciably.[12] In this work, fluorescence quenching of coptisine in the absence and presence of ctDNA by KI was used to determine the binding mode of coptisine to ctDNA (Figure 5). The fluorescence quenching data was analyzed using the well-known Stern–Volmer equation[23]

$$\frac{F_0}{F} = 1 + K_{SV}[Q] \quad (1)$$

Where F_0 and F denote the steady–state fluorescence intensities in the absence and in the presence of quencher (coptisine), respectively, K_{SV} is the Stern–Volmer quenching constant and $[Q]$ is the concentration of the quencher. Hence, equation (1) was applied to determine K_{SV} by linear regression of a plot of F_0/F against $[Q]$. The Stern–Volmer plots for the coptisine quenched by the KI in the absence and presence of ctDNA (Figure 5), were used to tabulate the values of quenching constants (K_{SV}) (Table1). It was apparent that the negatively charged quenching effect was decreased with addition of coptisine, further evidence in support of coptisine molecules intercalating into the base pairs of ctDNA.

3.4 Quenching Mechanism

Fluorescence quenching is usually classified as either dynamic or static and can be distinguished by their differing dependence on temperature and viscosity.[24] Higher temperatures will typically result in faster diffusion and increase collision efficiency, hence larger amounts of collisional quenching. In this work, the effect of temperature on ctDNA−AO−coptisine fluorescence quenching was studied.

Figure 6 displays the Stern–Volmer plots of the quenching of ctDNA−AO system fluorescence by coptisine at different temperatures (292, 298, 304, and 310 K). The corresponding Stern–Volmer quenching constant at different temperatures are shown in Table 2. These results indicate that the probable fluorescence quenching mechanism of the ctDNA−AO system by coptisine was a dynamic quenching process, because the K_{SV} increased with increasing temperature. This phenomenon demonstrated that the binding process between ctDNA with coptisine was a dynamic collision process.

The interaction forces between drugs and biomolecules may include electrostatic interactions, multiple hydrogen bonds, van der Waals interactions, as well as hydrophobic and steric contacts within the antibody−binding site. To elucidate the thermodynamic parameters of the interaction between coptisine and ctDNA, the Arrhenius equation was used to calculate the activation energy E_a [25]

$$\ln K_{SV} = -\frac{E_a}{RT} + \ln A \qquad (2)$$

Where K_{SV} is the Stern−Volmer quenching constant at the corresponding temperature, A is the pre-exponential, E_a is the apparent activation energy and R is the gas constant.

Figure 7 displays the Arrhenius plots of the quenching of ctDNA−AO system by coptisine at different temperatures, and the value of E_a is summarized in Table 2. The apparent activation energy E_a almost remained constant at different temperatures.

It is well known that pi-pi stacking is strong with a large enthalpy decrease. For intercalation, the DNA must undergo reorganization to a form that is more rigid and entropically less favorable.[26] Hence, the interaction of ctDNA and coptisine is enthalpy-driven. Van der Waals stacking interaction between the base pairs and the intercalated chromophore is the mainly force type in ctDNA-coptisine binding.[26]

One additional method to distinguish static and dynamic mechanism is by careful examination of the absorption spectra of the fluorophore as UV–vis absorption

measurements are a very simple and applicable method to investigate structural changes and complex formations.[27] Collisional quenching only affects the excited states of the fluorophores, and thus, no changes in the absorption spectra are expected. In contrast, ground-state complex formation will frequently result in perturbation of the absorption spectrum of the fluorophore.[28] In order to provide further evidence of the binding mechanism between ctDNA and coptisine being initiated by dynamic collision, we used difference absorption spectroscopy to obtain spectra. The absorption spectrum was obtained by subtracting the absorption spectrum of ctDNA from that of coptisine–ctDNA (1:1) complex at the same concentration (Figure 8, curve D) and the absorption spectrum of coptisine (Figure 8, curve A) was superimposed within experimental error. This was repeated for the absorption spectrum of ctDNA (Figure 8, curve B) and subtracting absorption spectra between ctDNA/coptisine 1:1 complex and coptisine (Figure 8, curve C). This result is additional support for a ctDNA-coptisine dynamic collision binding mechanism.

3.5 Effect of degeneration condition

The denaturant induced perturbation of the drug−DNA binding interaction was attempted to complement the aforementioned binding studies. Addition of denaturants leads to changes in the secondary and tertiary structure and conformational stability of biomacromolecules like DNA and proteins.[12] Urea, being a well-known denaturant, destabilizes the double stranded DNA helix and leads to the weakening drug−DNA interactions.[11] Urea was introduced to the coptisine-ctDNA system to investigate the influencing factors of binding. Figure 9 shows the changes in relative fluorescence intensity (F/F_0) for different concentrations of coptisine bound ctDNA at different urea:ctDNA ratios. These results demonstrated that, with increasing urea : ctDNA ratios

the relative degree of change in fluorescence intensity decreased, and the fluorescence intensity of coptisine–ctDNA system significantly decreased. This suggests that the urea-induced denaturation of ctDNA lead to the considerable weakening of the double stranded DNA helix, thereby weakening coptisine–ctDNA binding, resulting in the liberation of coptisine from the ctDNA environment. The results thus provide further evidence in support of the intercalative mode of coptisine–ctDNA binding.

3.6 Circular dichroism study

Conformational changes in DNA that are associated with small molecule binding can be detected efficiently by CD spectroscopy during drug−DNA interactions. The CD spectra of free ctDNA displays a positive band at 275 nm due to base stacking and a negative band at 246 nm due to right handed helicity, this is characteristics of the canonical B−form conformation of ctDNA, with any changes in the CD spectra atributable to the corresponding changes in ctDNA structure.[29] As reported, earlier DNA binding of molecules at the grooves or electrostatic interactions do not greatly impact the CD signal, whereas intercalative binding affects both the positive and negative bands.[29–31] Gradual addition of coptisine to the ctDNA solution reveals a significant decrease in signal intensity of the negative band in the ctDNA CD spectra, coupled with slight changes in the positive band signal (Figure 10), which indicates that the binding of the coptisine molecule with ctDNA did disturb the right handed helicity, although not extensively. This study indicated that coptisine interacted with the ctDNA and significantly perturbed base pair stacking, but not the gross helical ctDNA structure.

3.7 Electrochemistry

The application of electrochemical methods to the study of drug with macromolecule

interactions endows with a useful complement to the previously used techniques.[11,32] Considering the redox active sites of coptisine, drug binding to DNA may result in considerable alteration of redox properties. In a cyclic voltammetric (CV) study, changes in the current and potential of the ctDNA modified gold electrode in the absence and the presence of coptisine at room temperature (T = 298 K) are presented in Figure 11 (a, b, c). With a gradual increase in coptisine concentration, changes in cyclic voltammograms were obviously at the previous three or four times, the values of peak current i_p (Figure 11 (b)) were showed obviously increase at the previous three or four times. The increased peak current indicated that the binding of coptisine with ctDNA promotes the process of oxidation and reduction on the electrode surface.[33] After repetition, experiment results showed that a change in either the drug concentrations or the ctDNA concentrations would result in the same variation tendency at the previous three or four times.

In addition, electrochemical impedance spectroscopy (EIS) was also used to characterize the interfacial resistance change during the binding process of coptisine with ctDNA. Prominent decreases in diameter of the semicircle in the Nyquist plots were observed (Figure 12) at the previous three times upon the coptisine binding with ctDNA modified on the surface of electrode. This phenomenon demonstrated that the binding of coptisine with ctDNA can promote electron transfer on the electrode surface.[34]

These experiments together with the changes in CV and EIS confirmed that the mechanism of this interaction process was predominantly a dynamic process. As such, the effect of altering the reaction temperature on the binding of coptisine with ctDNA was studied. Figure 13 (a, b, c) displays the change in the cyclic voltammogram with increasing reaction temperature, with constant coptisine and ctDNA concentrations. The

peak current increased with increasing temperature (Figure 13). These results further illustrate that reaction temperature can greatly influence the binding dynamic binding of coptisine with ctDNA.

3.8 Molecular modeling

Molecular docking has shown great promise as a promising tool for the discovery of small molecule drugsfor targeting macromolecules.[35] In this study, molecular docking of coptisine with ctDNA was performed to obtain an insight with regards to the binding site and binding location in the DNA environment, along with the preferred orientation of the interactions between DNA and coptisine. Here, the 3D crystal structure of B-DNA used for docking was extracted from the RCSB Protein Data Bank (PDB), identifier 1Z3F. The predicted binding model with the lowest docking energy was then selected for binding orientation analysis. The best docked model (Figure 14) revealed that coptisine intercalative binding to the DNA double helix occurs via non-covalent stacking interactions with DNA base pairs, consistent with the aforementioned experimental results. DNA intercalators are mostly polycyclic, aromatic, and planar, with the intercalation with DNA considered as a specific variety of aromatic stacking interactions.[36] In our case, coptisine is a simple polycyclic aromatic molecule without side chains, and the space structure of coptisine is considered a classic rigid plane when subjected to energy optimization. Thus, coptisine interacts with DNA double helix between two adjacent base pairs in the DNA strand, forming stable sandwich-like structures. As a result, intercalation leads to localized perturbations to the DNA double helix. It opens a space between base pairs and unwinds the helical twist considerably. The result further validated the conformational changes in CD spectrum, and conclusions drawn for spectroscopic experiments.

4. Conclusions

In this work, the combination of spectral deciphering with electrochemical and molecular modeling methods unveiled the interaction of coptisine with ctDNA. The collective results are strongly indicative of a predominantly dynamic and intercalative coptisine DNA-binding mode, where the binding reaction is spontaneous and van der Waals stacking interaction is the mainly force type. Furthermore, the results indicate that coptisine exhibits DNA binding properties compatible with a prospective use as an efficient DNA probe. This report provides the foundations for further development of coptisine analogs for pharmacological applications.

Acknowledgments

This work was supported by the National Natural Science Foundation of China (No. 21273065), and the Research Foundation of Education Bureau of Hubei Province, China (No. Q20122205).

References

1 J. H. Schrittwieser and V. Resch, The role of biocatalysis in the asymmetric synthesis of alkaloids, *RSC Adv.,* 2013, **3**, 17602−17632.

2 L. Grycová, J. Dostál and R. Marek, Quaternary protoberberine alkaloids, *Phytochemistry,* 2007, **68**, 150−175.

3 C. Jash and G. S. Kumar, Binding of alkaloids berberine, palmatine and coralyne to lysozyme: a combined structural and thermodynamic study, *RSC Adv.,* 2014, **4**, 12514–12525.

4 D. Yu, S. L. Fu, Z. F. Cao, M. M. Bao, G. C. Zhang,Y. Y. Pan, W. M. Liu and Q. S. Zhou, Unraveling the novel anti–osteosarcoma function of coptisine and its mechanisms, *Toxicol. Lett.,* 2014, **226***,* 328–336.

5 L. H. Liu, and Z. L. Chen, Analysis of four alkaloids of coptis chinensis in rat plasma by high performance liquid chromatography with electrochemical detection, *Anal. Chim. Acta,* 2012, **737***,* 99–104.

6 J. Tang, Y. B. Feng, S. Tsao, N. Wang, R. Curtain and Y. W. Wang, Berberine and coptidis rhizoma as novel antineoplastic agents: a review of traditional use and biomedical investigations, *J. Ethnopharmacol.,* 2009, **126***,* 5–17.

7 S. Hiroka, T. Hiroki, M. Hajime and I. Makoto, Differential gene expression in rat vascular smooth muscle cells following treatment with coptisine exerts a selective antiproliferative effect, *J. Nat. Prod.,* 2011, **74***,* 634–638.

8 G. Q. Wang, Y. F. Qin, L. M. Du, J. F. Li, X. Jing, Y. X. Chang and H. Wu, Determination of amantadine and rimantadine using a sensitive fluorescent probe, *Spectrochim. Acta, Part A,* 2012, **98***,* 275–281.

9 C. F. Li, L. M. Du, W. Y. Wu and A. Z. Sheng, Supramolecular interaction of cucurbit [n] urils and coptisine by spectrofluorimetry and its analytical application, *Talanta,* 2010, **80***,* 1939–1944.

10 Z. H. Zhang, A. J. Deng, L. Q. Wu, L. H. Fang, J. Q. Yu, Z. H. Li, T. Y. Yuan, W. J. Wang, G. H. Du and H. L. Qin, Syntheses and structureeactivity relationships in cytotoxicities of 13–substituted quaternary coptisine derivatives, *Eur. J. Med. Chem.,* 2014, **86***,* 542−549.

11 S. M. Soumya, S. R. Somnath, C. Sayantani, B, Sudin and C. B. Subhash, Unveiling the groove binding mechanism of a biocompatible naphthalimide–based organoselenocyanate with calf thymus DNA: an “Ex Vivo” fluorescence imaging

application appended by biophysical experiments and molecular docking simulations, *J. Phys. Chem. B,* 2013**, 117***,* 14655–14665.

12 J. Barnali, S. Sudipta, G. Debanjana, B. Debosreeta and C. Nitin, Spectroscopic exploration of mode of binding of ctDNA with 3−hydroxyflavon e: a contrast to the mode of binding with flavonoids having additional hydroxyl groups, *J. Phys. Chem. B,* 2012, **116***,* 639–645.

13 Y. R. Cui, E. J. Hao, G. Q. Hui, W. Guo and F. L. Cui, Investigations on the interactions of diclofenac sodium with HSA and ctDNA using molecular modeling and multispectroscopic methods, *Spectrochim. Acta, Part A,* 2013**, 110***,* 92–99.

14 S. Selvaraj, S. Krishnaswamy, V. Devashya, S. Sethuraman and U. M. Krishnan, Synthesis, characterization and DNA binding properties of rutin–iron complex, *RSC Adv.,* 2012, **2,** 2797–2802.

15 H. D. Chen, G. Y. Chen, F. Du, Q. Q. Fu, Y. Zhao and Z. Tang, DNA display for drug discovery, *RSC Adv.,* 2013, **3,** 16251–16254.

16 X. L. Li, Y. J. Hu, H. Wang, B. Q. Yu and H. L. Yue, Molecular spectroscopy evidence of berberine binding to DNA: comparative binding and thermodynamic profile of intercalation, *Biomacromolecules,* 2012, **13,** 873–880.

17 X. Y. Su, L. Kong, X. Li, X. G. Chen, M. Guo and H. F. Zou, Screening and analysis of bioactive compounds with biofingerprinting chromatogram analysis of traditional Chinese medicines targeting DNA by microdialysis/HPLC, *J. Chromatogr. A,* 2005, **1076**, 118–126.

18 Sybyl Software, St. Louis, Tripos Associates Inc., MO, USA.

19 S. Muhammad, A. Saqib and B. Amin, Drug–DNA interactions and their study by UV–Visible, fluorescence spectroscopies and cyclic voltametry, *J. Photoch. Photobio. B,* 2013, **124***,* 1–19.

20 E. C. Long and J. K. Barton, On demonstrating DNA intercalation, *Acc. Chem. Res.,* 1990, **23,** 271–273.

21 Y. Zhang, Z. Q. Xu, X. R. Liu, R. L. Liu, Z. D. Qi, F. L. Jiang and Y. Liu, Conformation and thermodynamic properties of the binding of vitamin C to human serum albumin, *J. Solution Chem.,* 2012, **41,** 351−366.

22 H. K. Liu and P. J. Sadler, Metal complexes as DNA intercalators, *Acc. Chem. Res.,* 2011, **44**, 349–359.

23 R. J. Lakowicz, Principles of fluorescence spectroscopy, 3rd ed. *Springer,* New York, 2006.

24 Z. X. Chi and R. T. Liu, Phenotypic characterization of the binding of tetracycline to human serum albumin, *Biomacromolecules,* 2011, **12,** 203–209.

25 J. L. Keith, The development of the Arrhenius equation, *J. Chem. Educ.,* 1984, **61,** 494.

26 J. B. Chaires, Calorimetry and thermodynamics in drug design, *Annu. Rev. Biophys.,* 2008, **37**, 135−51.

27 Y. J. Hu, Y. Liu, X. S. Shen, X. Y. Fang and S. S. Qu, Studies on the interaction between 1–hexylcarbamoyl–5–fluorouracil and bovine serum albumin, *J. Mol. Struct.,* 2005**, 738,** 143–147.

28 R. Mi, B. Tu, X. T. Bai, J. Chen, Y. Ouyang and Y. J. Hu, Binding properties of palmatine to DNA: spectroscopic and molecular modeling investigations, *Luminescence,* 2015, DOI 10.1002/bio.2904.

29 M. Anamika and C. Sankar, Modification of a styryl dye binding mode with calf thymus DNA in vesicular medium: from minor groove to intercalative, *J. Phys. Chem. B,* 2012, **116**, 5226−5233.

30 K. Suman, K. B. Manas, B. Ananya, B. Kakali, S. K. Gopinatha, G. B. D. Michael, B.

Ranjan and G. Prasanta, Synthesis, structure and DNA binding studies of 9-phenyldibenzo [a, c] phenazin-9-ium, *RSC Adv.,* 2013, **3**, 3054–3061.

31 Y. Zahid, R. B. Abdul, A. H. Mohammed, T. Mohammad and U. D. Kabir, Determination of the cationic amphiphilic drug–DNA binding mode and DNA-assisted fluorescence resonance energy transfer amplification, *Spectrochim. Acta, Part A,* 2014, **122**, 553–564.

32 S. Huang, F. W. Zhu, Q. Xiao, Q. Zhou, W. Su, H. N. Qiu, B. Q. Hu, J. R. Sheng and C. S. Huang, Combined spectroscopy and cyclic voltammetry investigates the interaction between [(η6-*p*-cymene)Ru(benzaldehyde-N(4)-phenylthiosemicarbazone)Cl]Cl anticancer drug and human serum albumin, *RSC Adv.,* 2014, **4**, 36286–36300.

33 B. Cheng, X. Q. Cai, Q. Miao, Z. H. Wang and M. L. Hu, Selective interactions between 5−fluorouracil prodrug enantiomers and DNA investigated with voltammetry and molecular docking simulation, *Int. J. Electrochem. Sci.,* 2014, **9**, 1597–1607.

34 C. Y. Yin, G. S. Lai, L. Fu, H. L. Zhang and A. M. Yu, Ultrasensitive immunoassay based on amplified inhibition of the electrochemical stripping signal of silver nanocomposite by silica nanoprobe, *Electroanalysis,* 2014, **26**, 1–7.

35 B. Tu, Z. F. Chen, Z. J. Liu, L. Y. Cheng and Y. J. Hu, Interaction of flavones with DNA in vitro: structure–activity relationships, *RSC Adv.,* 2015, **5**, 33058–33066.

36 S. Li, V. R. Cooper, T. Thonhauser, B. I. Lundqvist and D. C. Langreth, Stacking interactions and DNA intercalation, *J. Phys. Chem. B,* 2009, **113,** 11166–11172.

Figure captions

Figure 1. Molecular structure of coptisine.

Figure 2. UV absorption spectra of ctDNA with various concentrations of coptisine. Inset: Comparison of absorption at 260 nm between the ctDNA–coptisine complex and the sum values of circular ctDNA and coptisine. c (ctDNA) = 1.0×10^{-4} mol·L^{-1}; c(coptisine)/(10^{-5}mol·L^{-1}), A–K: from 0 to 20.0 at increments of 2.0.

Figure 3. Fluorescence spectrum of ctDNA with various concentrations of coptisine. Inset: Relative fluorescence intensity for ctDNA as a function of the coptisine for different concentrations. c (ctDNA) = 1.0×10^{-5}mol·L^{-1}; c (coptisine)/(10^{-6} mol·L^{-1}), A–K: from 0.5 to 12.5 at increments of 0.5.

Figure 4. Fluorescence spectrum of ctDNA–AO with various concentrations of coptisine. The inset corresponds to the Stern–Volmer plots. c (ctDNA) = 1.0×10^{-4} mol·L^{-1}; c (AO) = 2.5×10^{-6} mol·L^{-1}; c (coptisine)/(10^{-5} mol·L^{-1}), A–Z: from 0.0 to 25.0 at increments of 1.0.

Figure 5. Fluorescence quenching of coptisine by I^- in the absence and presence of ctDNA. c (ctDNA) = 1.0×10^{-5} mol·L^{-1}; c (coptisine) = 1.0×10^{-5}mol·L^{-1}; c (I^-)/(10^{-3} mol·L^{-1}): from 0.0 to 25.0 at increments of 2.5.

Figure 6. Stern–Volmer plots of the coptisine–ctDNA (AO) system at different temperatures.

Figure 7. Arrhenius plot of the coptisine–ctDNA (AO) system.

Figure 8. The absorption spectrum of coptisine only (A: coptisine); the absorption spectrum of ctDNA only (B: ctDNA); the difference absorption spectrum between ctDNA-coptisine and coptisine (C: [ctDNA-coptisine]−[coptisine]); the difference

absorption spectrum between ctDNA-coptisine and ctDNA (D : [ctDNA-coptisine] − [ctDNA]). Conditions: *c* (ctDNA) = *c* (coptisine) = 1.0×10^{-4} mol·L^{-1}. pH = 7.4.

Figure 9. Plot of the variation in relative fluorescence intensity (F / F_0) of coptisine bound ctDNA with different amounts of denaturant. *c* (ctDNA) = 1.0×10^{-5} mol·L^{-1}. Inste: Effect of urea on the system of coptisine–ctDNA. *c* (ctDNA) = 1.0×10^{-5} mol·L^{-1}, *c* (coptisine) = 5.0×10^{-5} mol·L^{-1}, pH = 7.4.

Figure 10. Representative CD spectrum of ctDNA resulting from the interaction of coptisine, *c* (coptisine)/(10^{-7}mol·L^{-1}): from 0.0 to 10.0 at increments of 2.0.

Figure 11. (a) Cyclic voltammograms of ctDNA modified gold electrode with different concentrations of coptisine. (b) The values of peak current $i_{p,c}$ and $i_{p,a}$. (c) The values of peak potential $E_{p,c}$ and $E_{p,a}$.

Figure 12. Electrochemical impedance spectroscopy (EIS) of ctDNA modified gold electrode with different concentrations of coptisine.

Figure 13. (a) Cyclic voltammograms of ctDNA modified gold electrode with coptisine at different temperatures. (b) The values of peak current $i_{p,c}$ and $i_{p,a}$. (c) The values of peak potential $E_{p,c}$ and $E_{p,a}$.

Figure 14. Molecular modeling of the binding of coptisine to DNA. The coptisine molecule is shown as a cylinder model (C, gray; O, red; N, blue). Red hydrophobic surfaces indicate a strong electrostatic interaction, blue hydrophobic surface indicates a weak electrostatic interaction.

Tables

Table 1. The Quenching Effect of Negative Ion on the Coptisine–ctDNA Interaction

System	K_{SV}/(L·mol^{-1})	Decreased ratio
coptisine–I^-	68.6	79.9%
coptisine–ctDNA–I^-	13.8	

Table 2. Stern–Volmer Quenching Constants of Coptisine–DNA (AO) at Various Temperatures

pH	*T* (K)	$10^{-4}K_{SV}$/ (L·mol^{-1})	*R* [a]	*S.D.* [b]	E_a/ kJ·mol^{-1}
7.2	292	1.02	0.9990	0.0010	13.23
	298	1.14	0.9992	0.0010	
	304	1.28	0.9992	0.0012	
	310	1.39	0.9986	0.0016	

[a] ***R*** is the correlation coefficient. [b] ***S.D.*** is standard deviation.

Figure graphics

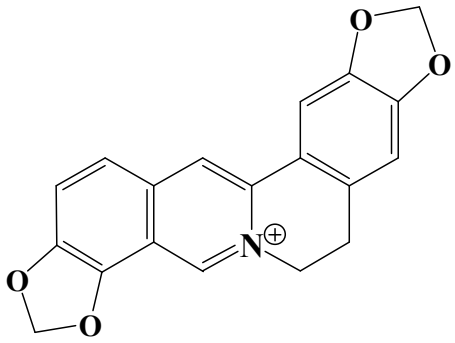

Figure 1

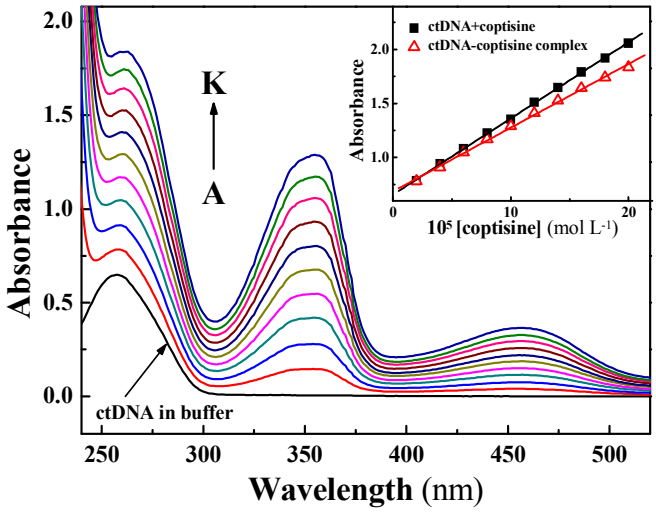

Figure 2

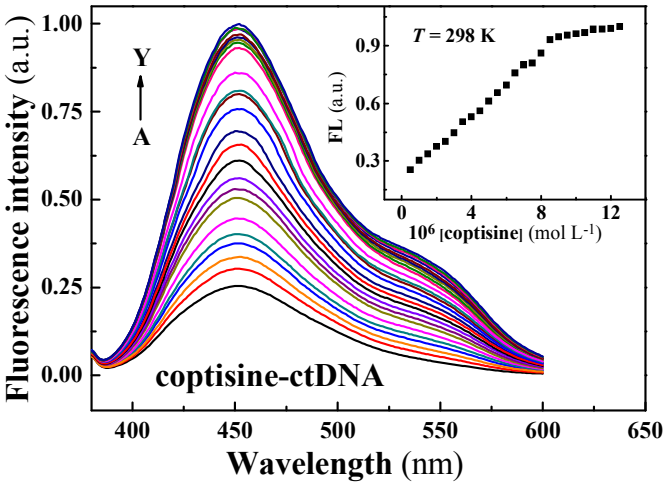

Figure 3

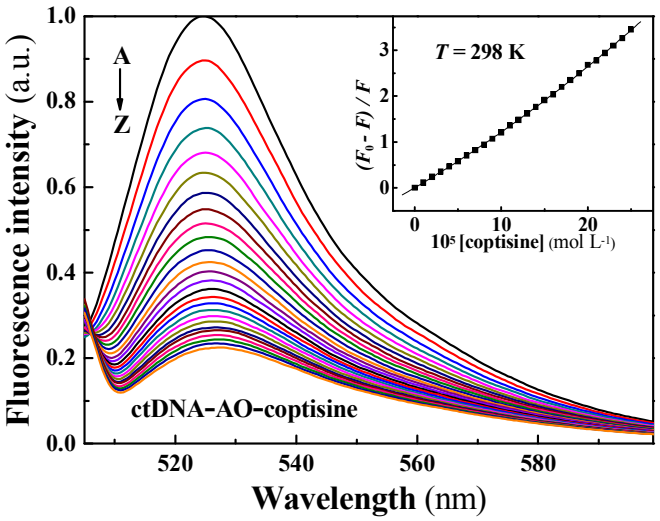

Figure 4

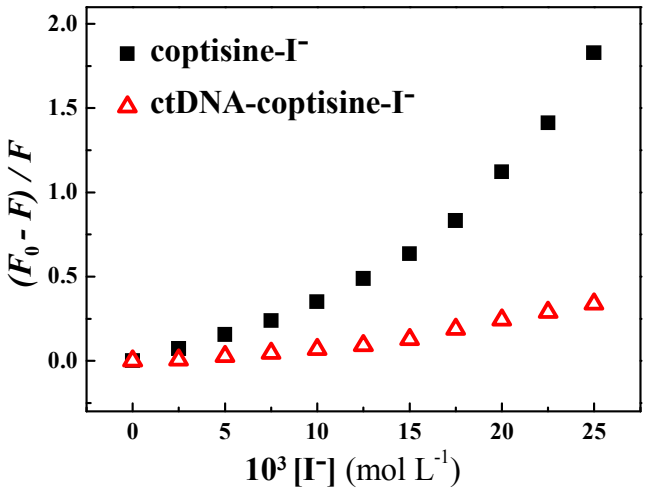

Figure 5

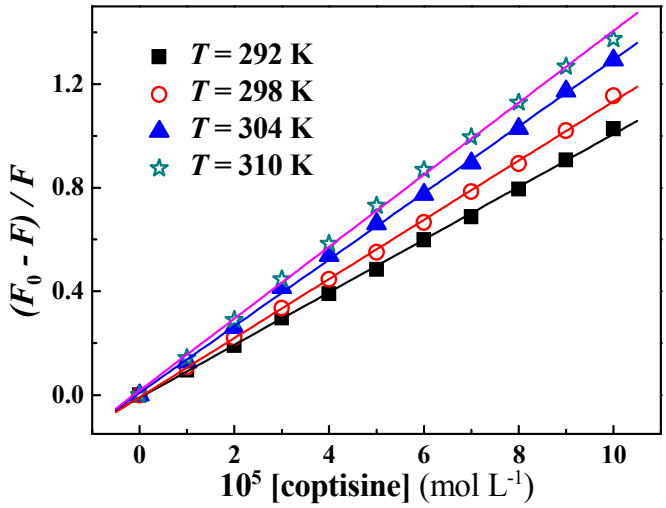

Figure 6

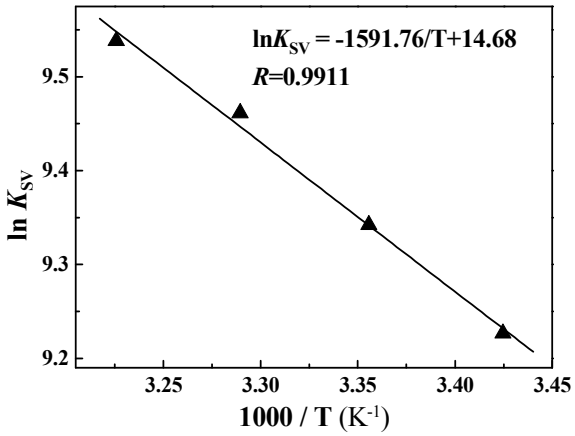

Figure 7

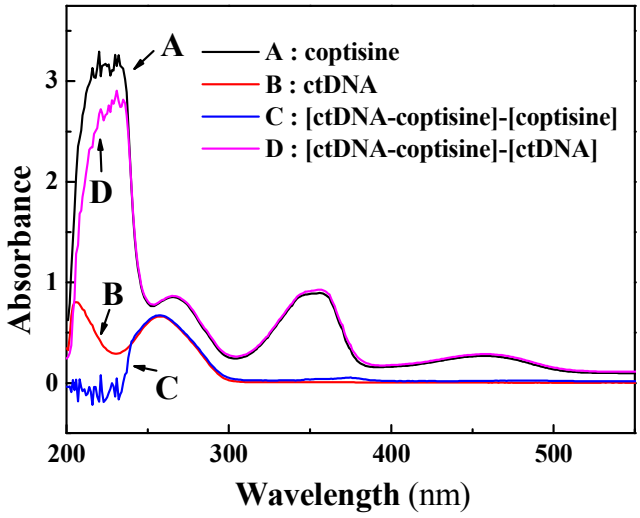

Figure 8

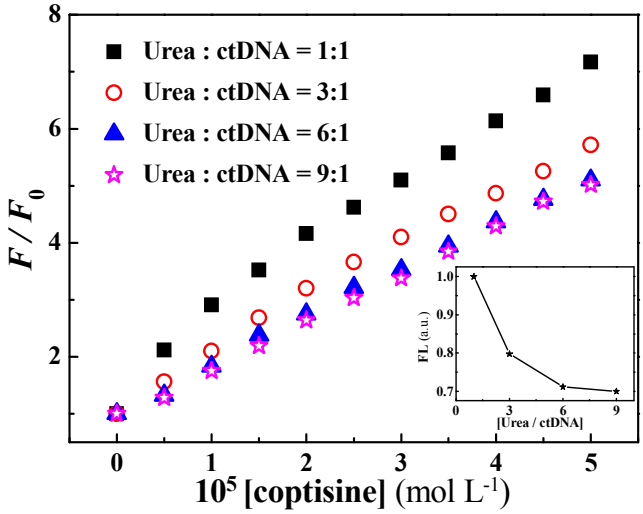

Figure 9

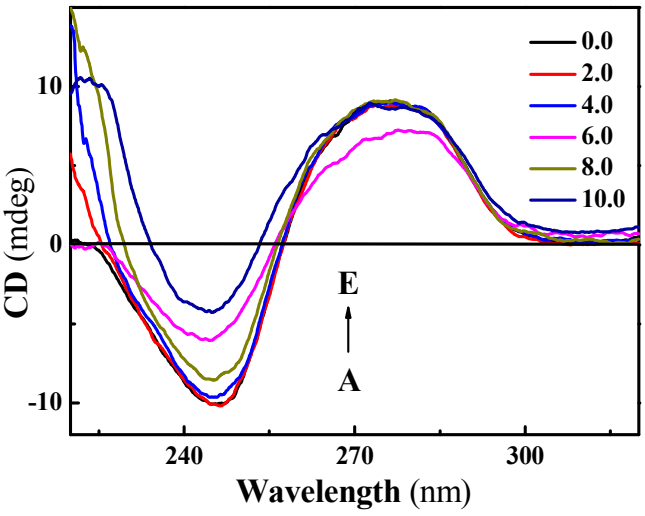

Figure 10

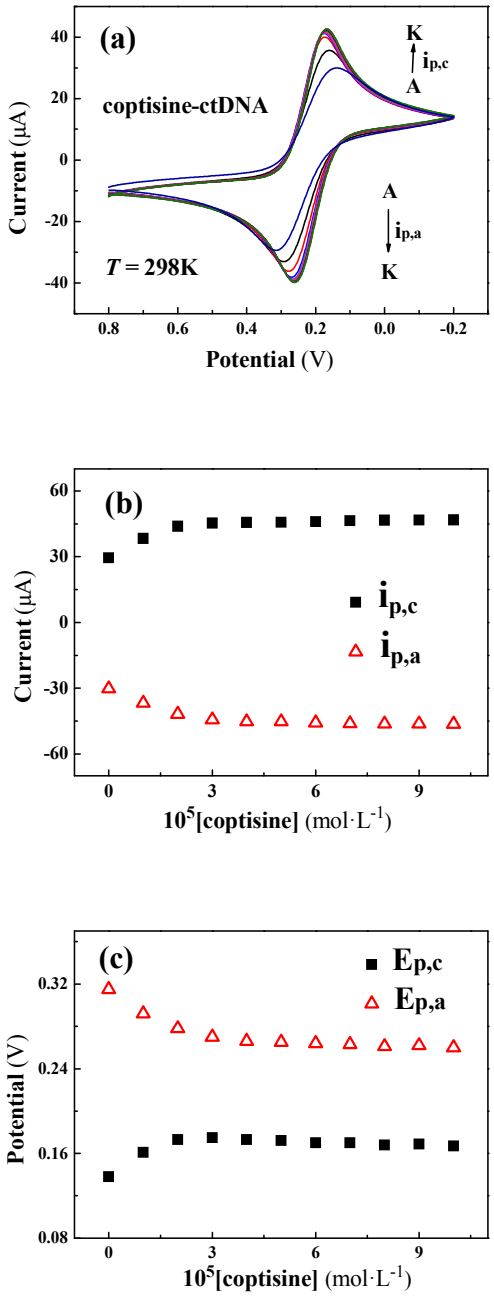

Figure 11

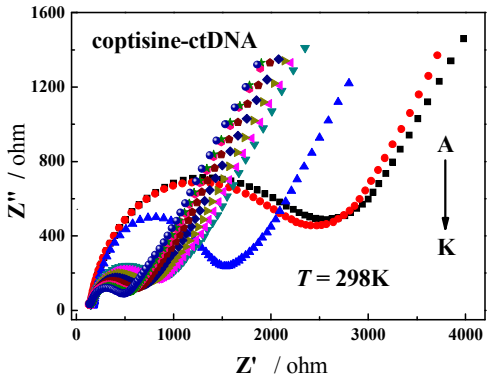

Figure 12

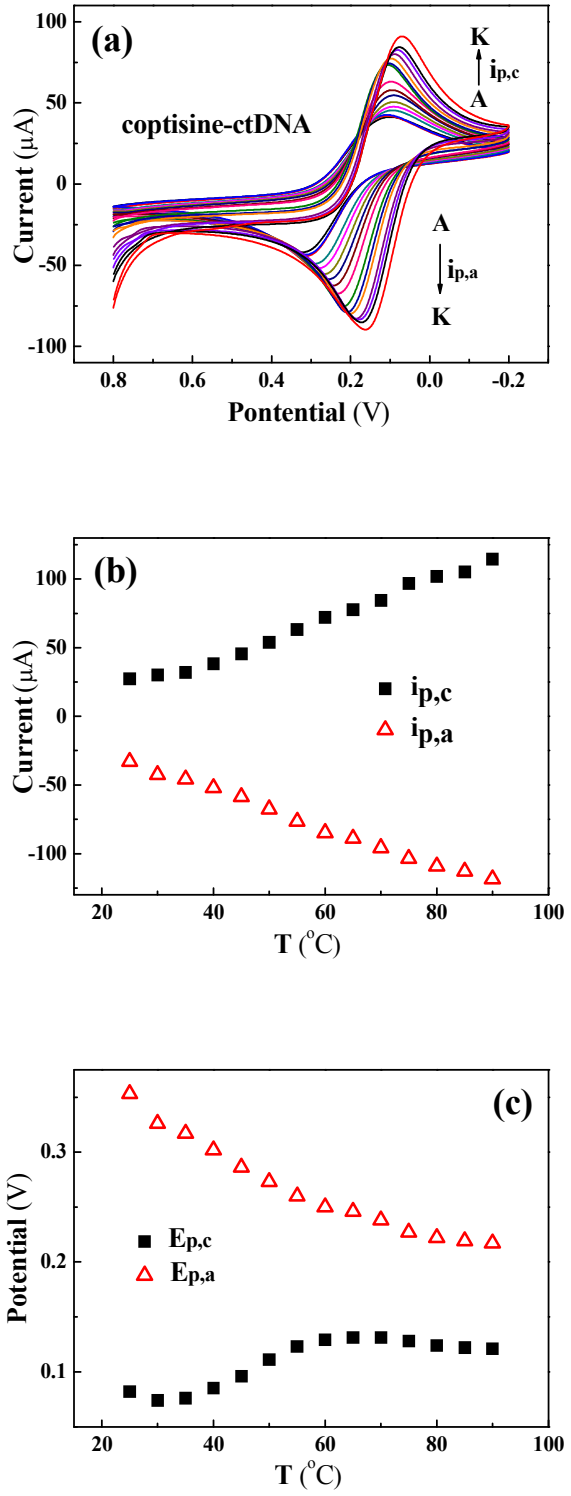

Figure 13

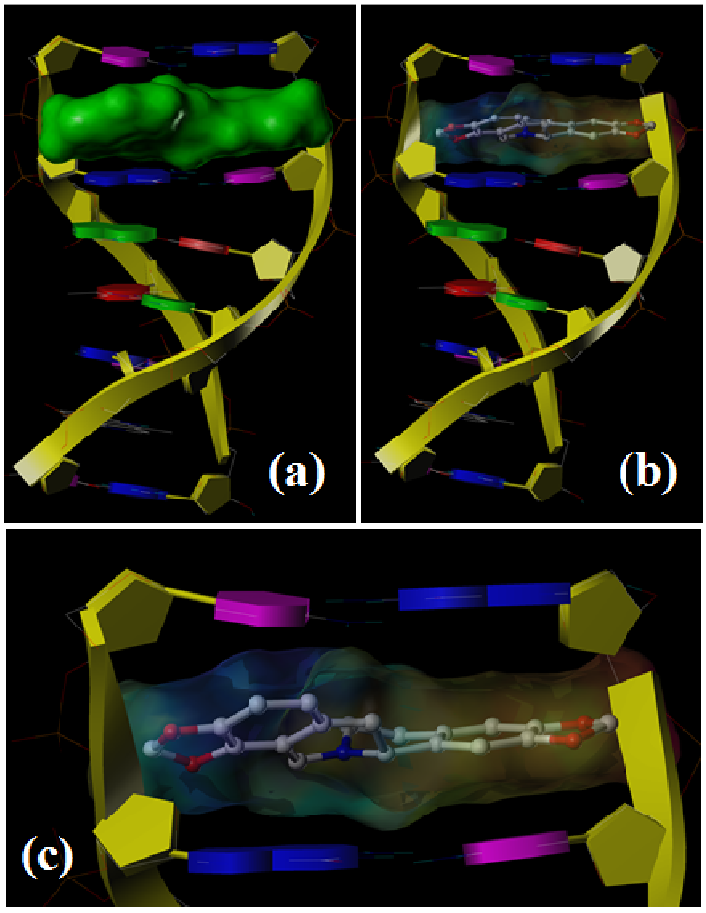

Figure 14